

A Paper Contributed to the Special Issue of the Chinese Journal of Physics
Celebrating Seventieth Birthday of Prof. Tn-You Wu

Positron Annihilation and Phase Transitions in Molecular Substances

S. Y. CHUANG(莊樹源)

*Physics Department, National Taiwan University
Taipei, Taiwan*

(Received July 10, 1978)

The technique of positron annihilation as applied to the study of phase transitions in molecular substances and polymers is reviewed. The emphasis is on the formation and annihilation of positronium atoms in condensed media. The annihilation rate of ortho-positronium in a medium is highly sensitive to microscopic structural changes which usually occur during phase transitions. The positron method is particularly valuable for the study of solid-solid phase changes, including the glass transition in polymers.

I. INTRODUCTION

POSITRON annihilation in condensed matter has been investigated extensively for more than twenty years. Earlier investigations are mainly on studies of annihilation processes of the positron and the formation of positron-electron bound states in condensed media. Since the First International Conference on Positron Annihilation, held in Detroit in 1965⁽¹⁾, positron annihilation has been used as a probe for the study of electron momentum distributions and other physical and chemical properties of materials. A more recent development has been the full recognition of the remarkable sensitivity of positrons to structure defects which leads to a new range of applications, such as determinations of vacancy formation energy in metals, studies of electron states in defects, studies of radiation damage, and detections of phase transitions.

Some recent review articles⁽²⁻⁵⁾ and Conference Proceedings^(1,6-8) have discussed in some details on a few areas such as studies of Fermi surface of metals and alloys, defects in solids as well as positronium chemistry. In this article, we shall focus our attention especially on the area of phase transitions investigated by the positron techniques. We shall first review briefly the general aspects of positron and positronium annihilation and discuss current experimental methods and theoretical models used in positron studies, especially in molecular substances. This is followed by a detailed discussion of recent positron works on phase changes in various molecular substances and polymers.

II. GENERAL BACKGROUND

The existence of positrons was first predicted by Dirac in 1930⁽⁹⁾, and was detected experiment-

- (1) A. T. Stewart and L. O. Roellig, ed., *Positron Annihilation* (Academic Press, New York, 1967).
- (2) R.N. West, *Adv. Physics* 22, 263 (1973).
- (3) I.Y. Dekhtyar, *Phys. ReP.9C*, 243 (1974).
- (4) S. Berko and J. Mader, *Appl. Phys.* 5, 287 (1975).
- (5) V.I. Goldanskii, *Atomic Energy Rev.* 6, 3 (1968).
- (6) B. G. Hogg and A.T. Stewart, ed., *Proc. of 2nd Int. Conf. on Positron Annihilation*, Kingston, Ontario, September 1971.
- (7) P. Hautajarvi and A. Seeger, ed., *Proc. of 3rd Int. Conf. on Positron Annihilation*, Ontaniemi, Finland, August 1973.
- (8) G. Trumphy, ed., *Proc. of 4th Int. Conf. on Positron Annihilation*, Helsingor, Denmark, August 1976.
- (9) P. A. M. Dirac, *Proc. Cambridge Phil. Soc.* 26, 361 (1930).

ally by Anderson during his observation of cosmic rays in 1932⁽¹⁰⁾. Later it was found that positrons not only were produced in cosmic ray showers but also could be created by gamma rays from radioactive sources⁽¹¹⁾. With the discovery of artificial radioactive β^+ emitter, more convenient sources of positrons became available. Since then the properties of the positron has been experimentally verified in considerable detail. The positron is the antiparticle of the electron. It has a mass equal to the electron mass. It carries one unit of positive charge and the spin 1/2. Annihilation of a positron upon collision with an electron can occur with the emission of gamma photons.

However, before annihilation takes place, a positron and an electron may form a bound system, called positronium (Ps). The possibility of bound positron-electron states was postulated by Mohorovicic in 1934⁽¹²⁾. The name of positronium was introduced by Ruark in 1945⁽¹³⁾. The first experimental demonstration of the existence of positronium was performed by Deutsch in 1951⁽¹⁴⁾. According to the simple Bohr model, in which the positronium atom is treated as the hydrogen atom with the exception that the reduced mass is one-half of the electron mass, the Bohr radius of a ground state positronium atom is 1.06 Å and the binding energy is 6.77 eV.

Positronium has two ground states. The singlet (1S_0) state with total spin zero is called para-positronium (p-Ps), and the triplet (3S_1) state with total spin one is called orthopositronium (o-Ps). Statistically, three-fourth of positronium formed is in the triplet state and the other one-fourth is in the singlet state. These two ground states are substantially different in their annihilation processes because of the existence of selection rules preventing the annihilation of the 3S state with the emission of only two photons⁽¹⁵⁾. From conservation of charge parity, the 1S state decays into an even number of photons and the 3S state into an odd number of photons. Since the probability of multiple-photon annihilation decreases greatly with increasing multiple, and since one-photon annihilation requires an external field, the singlet state decays into two photons and the triplet state undergoes three-photon decay. In free space the mean lifetimes of p-Ps and o-Ps are 1.25×10^{-10} sec and $1.4 \sim 10^{-7}$ sec, respectively. However, in a condensed medium, the meanlife of o-Ps is considerably reduced due to its interaction with surrounding molecules. There are three main processes which alter the meanlife of o-Ps in condensed media, namely, pick-off ortho-para conversion, and chemical quenching. Pick-off is the annihilation of the positron in the o-Ps atom with an atomic or molecular electron of opposite spin at the moment of collision. If the surrounding molecules contain unpaired electrons, o-Ps can be converted into p-Ps with subsequent rapid two-photon decay. This is called ortho-para conversion. It is also possible for o-Ps atoms to undergo chemical reactions with other molecules, especially chemically active molecules and free radicals, and to form positronium compound which annihilate rapidly via two-photon decay. This process of shortening o-Ps lifetime is called chemical quenching. In normal molecular substances, pick-off annihilation is the most common decay process of o-Ps. A flow diagram describing the fate of the positron in condensed media is shown in Fig. 1.

III. EXPERIMENTAL METHODS

A. Lifetime Measurements

There are three main methods by which information on positron annihilation in a substance may be gained. The first of these is through the measurement of the mean lifetimes of the annihilating positrons. Two types of annihilation parameters are found in experiments of this kind, first the decay rates for the various processes by which positrons can annihilate and second the fraction of positrons decaying by each of the different modes. By use of this method one is able to obtain information concerning electronic and structural properties of the sample, because both the decay rates and the relative intensity of positrons decaying by the different decay modes are closely related to these properties.

(10) C.D. Anderson, Phys. Rev. 41, 405 (1932).

(11) P.M.S. Blackett, J. Chadwick, and G.P.S. Occhialini, Proc. Roy. Soc. (London) A 44, 235 (1934).

(12) S. Mohorovicic, Astron. Nachr. 253, 94 (1934).

(13) A.E. Ruark, Phys. Rev. 68, 278 (1945).

(14) M. Deutsch, Phys. Rev. 82, 455 (1951).

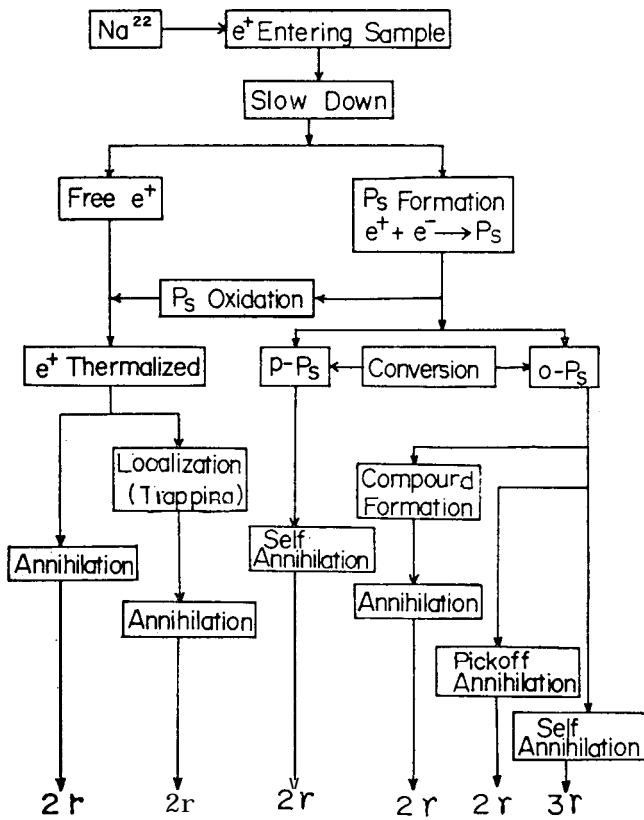


Fig. 1. Flow diagram of positron annihilation processes in molecular substances

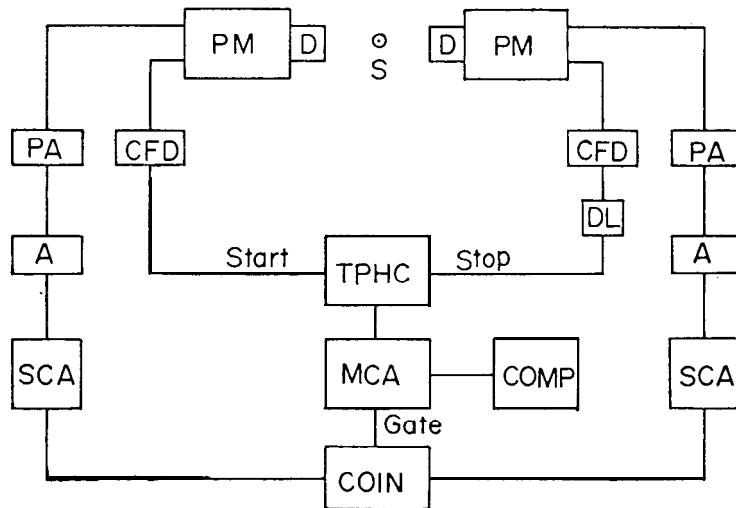


Fig. 2. A typical system for lifetime measurements.

- | | |
|-------------------------------------|-------------------------------|
| S-Source and Sample | A-Amplifier |
| D-Plastic Scintillator | SCA-Single-Channel-Analyzer |
| PM-Photomultiplier | COIN-Coincidence Unit |
| CFD-Constant Fraction Discriminator | MCA-Multiple-Channel-Analyzer |
| TPHC-Time-to-Pulse-Height Converter | COMP-Computer |
| PA-Pre-amplifier | |

A typical system for measuring positron lifetimes is shown in Fig. 2. The radioactive isotope ^{22}Na is used as the positron source because it emits a positron and, almost simultaneously, a 1.28 MeV nuclear gamma-ray which can be used as the start signal of the birth of a positron. Annihilation of the positron is signaled by 0.51 MeV annihilation gamma rays. The time delay between these two events, the lifetime of the positron, is measured by a fast-slow coincidence technique. A pair of fast photomultiplier tubes (RCA 8575) coupled with plastic scintillators (NATON-136) are used as detectors. One is set to receive only 1.28 MeV photons (start signals) and the other accepts 0.51 MeV photons (stop signals). The time between the start and stop signals is converted into an electrical pulse by a time-to-pulse-height converter (TPHC). The amplitude of the pulse from the output of TPHC is proportional to the time interval. This analog signal is stored in a multichannel analyzer (MCA) according to its height. Data stored in MCA are then analyzed by computer to determine the meanlife and the relative intensity of each component associated with various decay modes of positrons. A typical lifetime spectrum is shown in Fig. 3. The lifetime spectrum consists of a sum of decaying exponentials and a constant background. Because of the finite resolution of the equipment, the spectrum is rounded at the top. The spectrum can be analyzed by using the method of least-square fitting. The meanlife, τ , of each lifetime component is calculated from the exponential decay rate of that component. The area under the component divided by the total area of the spectrum is called the relative intensity, I , of the component. Each component has its own characteristic values of τ and I depending on the properties of the sample.

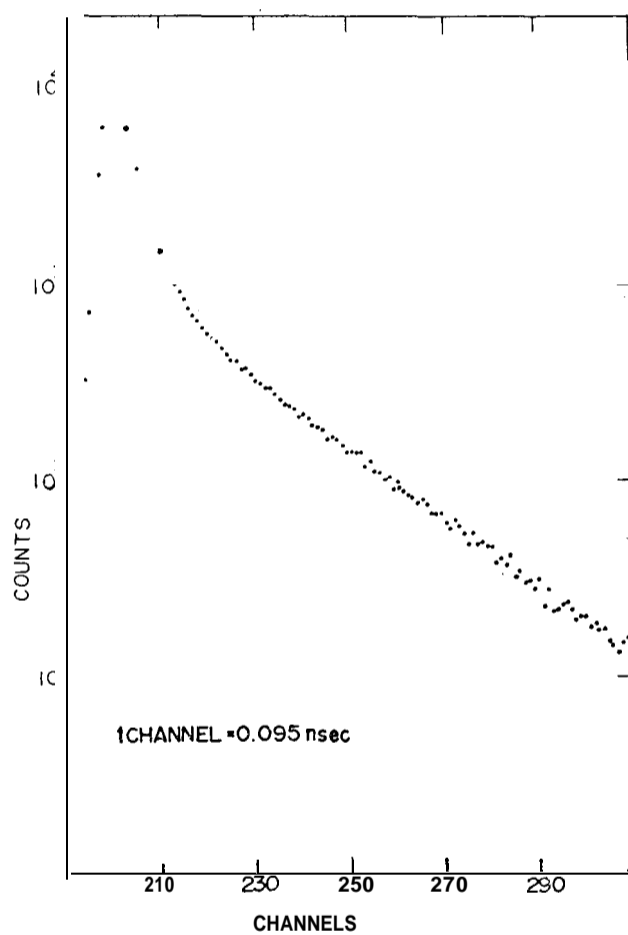


Fig. 3. A typical lifetime spectrum.

B. Angular Correlation Experiments

The second method of studying positron annihilation is through the measurement of the angular correlation of the two-photon annihilation radiation. When a positron-electron pair annihilates at rest, two photons are emitted in opposite directions, each with a momentum of the order of mc . If now the annihilating pair has a momentum \mathbf{p} at the time of annihilation, then the photon pair will be emitted at an angle deviated from 180 degrees by an amount of p_{\perp}/mc in the laboratory frame, where p_{\perp} is the momentum component perpendicular to the emission direction of the annihilating photons. Thus by measuring the angular distributions of the annihilating photons one is able to obtain the momentum distribution of the annihilating pairs. The angular correlation method can also be used to identify the presence of the annihilation of p-Ps because it gives a narrow (low momentum) peak which is quite different from the broad momentum distribution produced by direct annihilation of free positrons and the pick-off annihilation of o-Ps. The conventional long slit angular correlation apparatus is shown in Fig. 4. It consists of a source of positrons (Na^{22} or Cu^{64}) and a sample mounted between a fixed and a movable detector with appropriate collimating slits. NaI(Tl) scintillators are most commonly used as detectors in this kind of experiments because of their good energy resolution and high efficiency. The collimating slits are usually with a slit width of 0.1-0.5 mrad depending on the requirement of the angular resolution. The detectors and the sample housing should be shielded properly and the coincidence resolution time should be short (e. g. 50 nsec) to maintain low background. The coincidence counts as a function of the angle θ which is the angle between the movable detector and the collimating line of the source and the fixed detector. The movable detector can be moved manually or it may be automated to sweep the coincidence counting rate in one direction, say z direction, within a predetermined range, e. g., from +20 mrad to -20 mrad. In the long slit type geometry, the detectors are made long in the y direction so that the measurements are proportional to

$$C(P_z) = \int_{-\infty}^{\infty} \int_{-\infty}^{\infty} \rho(\mathbf{p}) dp_x dp_y, \quad (1)$$

where $P_z \approx mc\theta$ and $\rho(\mathbf{p})$ is the momentum density of the annihilating positron-electron pair, or the probability of annihilation with an electron of initial momentum \mathbf{p} . In the independent particle approximation, $\rho(\mathbf{p})$ is

$$\rho(\mathbf{p}) = \left| \int \exp(-i\mathbf{p}\cdot\mathbf{r}) \varphi_+(\mathbf{r}) \varphi_-(\mathbf{r}) d\mathbf{r} \right|^2 \quad (2)$$

If the momentum distribution is isotropic, such as in gases, liquids, and amorphous or polycrystalline

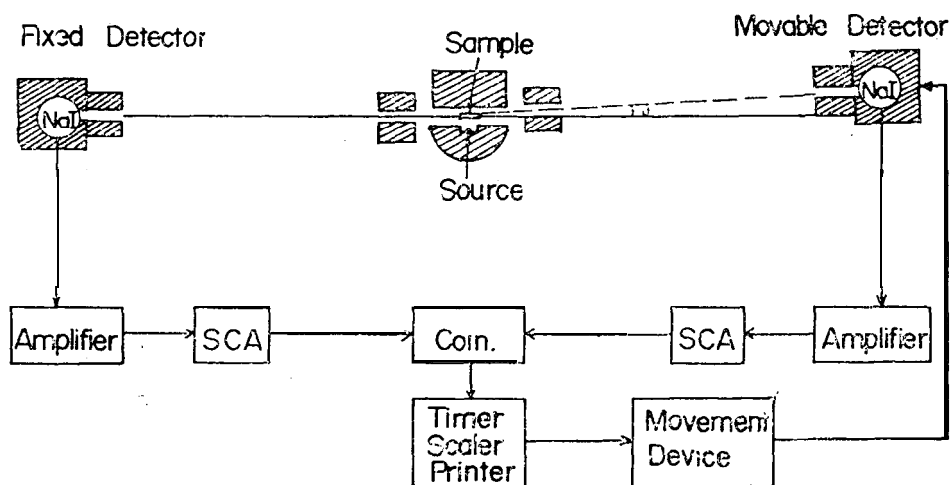


Fig. 4. The 2-r angular correlation apparatus

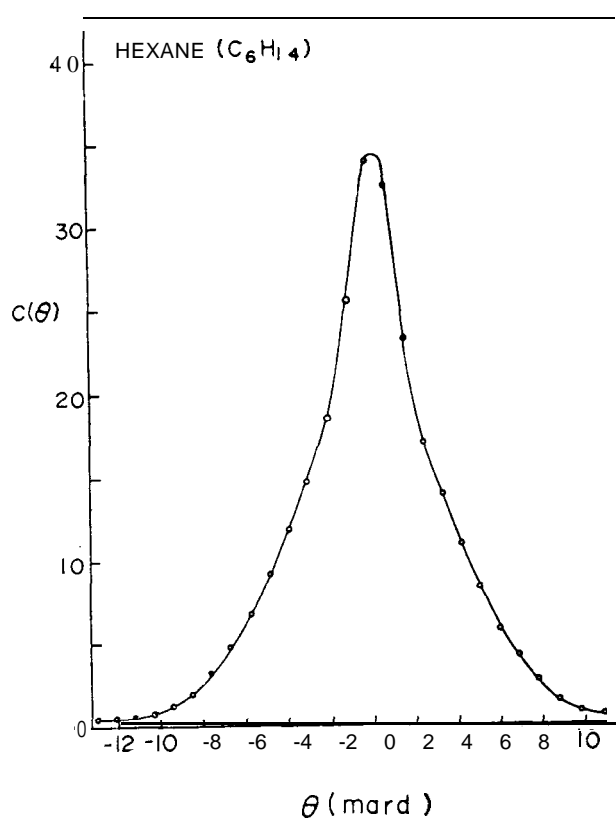


Fig. 5. Angular correlation distributions $C(\theta)$ for hexane

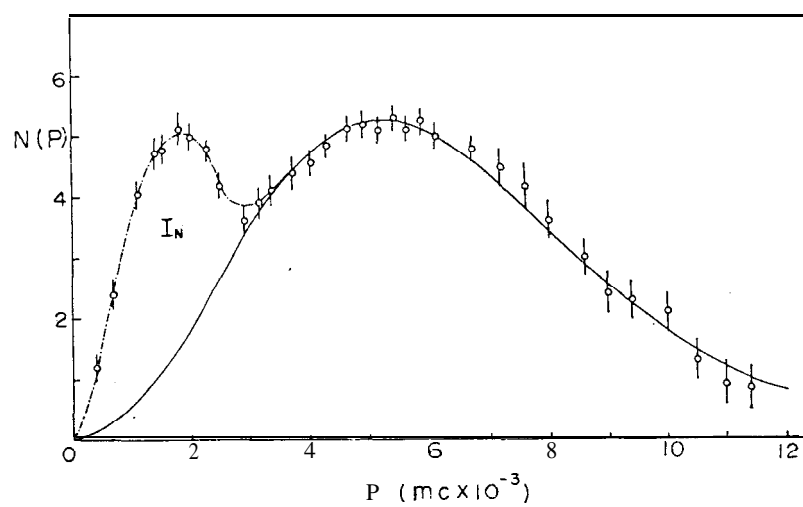


Fig. 6. Momentum distributions $N(P)$ for hexane

solids, the experimental data can also be presented in the form of $p(p)$ or $N(p)$ by the following conversion¹,

$$\rho(p) = \text{const.} \cdot \frac{1}{p_z} \cdot \frac{dC(p_z)}{dp_z} \quad (3)$$

$$N(p) = \text{const.} \cdot p_z \cdot \frac{dC(p_z)}{dp_z} \quad (4)$$

A typical angular correlation curve $C(\theta)$ and its corresponding momentum distribution $N(p)$ are shown in Fig. 5 and 6 respectively.

C. The Doppler Broadening Technique

The third method is through the measurement of the energy difference of annihilation photons due to the Doppler effect. This technique measures the longitudinal component of the photon pair momentum. A sensible measurement of Doppler-broadening lineshapes can only be made with a modern solid state detector. The experimental arrangement for detecting the Doppler effect is quite simple. A positron source is placed next to the sample and the emitted photons are analyzed by a Ge or Ge(Li) detector as shown in Fig. 7. The resolution of the momentum distribution obtained by this method is not as good as the one obtained from the angular correlation method. Therefore, deconvolution of the resolution is essential in this case⁽¹⁵⁾. A typical Doppler-broadening spectrum, with and without deconvolution of the resolution, is shown in Fig. 8. However, there is an advantage for using this method because it only takes a couple of hours to accumulate a spectrum with a weak source (10 μCi). The angular correlation method even with a much stronger source (10 mCi) needs a few days to accumulate an equivalent spectrum. Another advantage of using a weaker source is that the radiation damage in the sample is negligible. Using a stronger source some time will induce defects in the sample. For example, crystals of alkali halides change their color after one day of exposure with 10 mCi of Na^{22} (or Cu^{64}) which is the normal radioactivity used in the angular correlation experiment. In such case, the Doppler broadening technique is better than the angular correlation method.

There are two basic approaches, the basic science approach and the technological approach, commonly used in analyzing of positron data. The former approach is to analyze the positron data in as detailed a manner as possible in order to correlate the various experimental parameters, such as various lifetime components and momentum components, with specific microscopic properties of the sample. The technological approach is to establish the correlation between a certain portion of the positron data and some macroscopic properties of the sample without detailed analysis of various parameters. For example, the area under the central portion of the Doppler spectrum or the angular correlation spectrum divided by the total area of the spectrum reflects the fraction of positron annihilation with low center-of-mass momentum such as from self-annihilation of p-Ps. Therefore, one

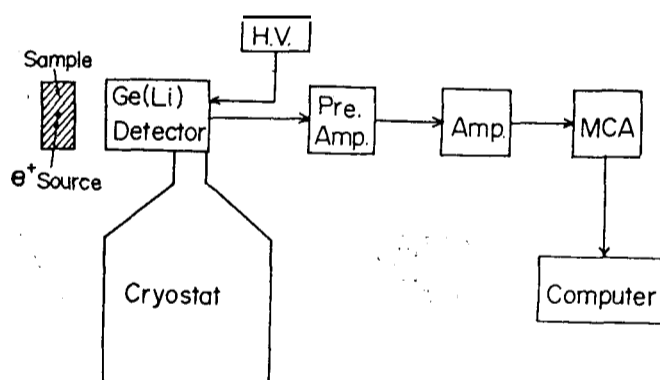


Fig. 7. A block diagram of Doppler-broadening experiment.

(15) S. Dannefaer and D. P. Kerr, Nucl. Inst. Meth. 131, 119 (1975).

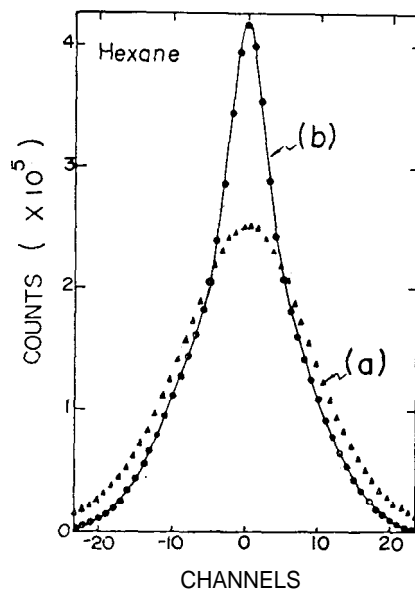


Fig. 8. Doppler broadened spectrum for hexane: (a) raw data
(b) deconvoluted⁽¹⁵⁾.

can still obtain useful information by comparing the above mentioned sample parameter with macroscopic material property, such as sample temperature, without knowing the detailed shape of the momentum distributions. The technological approach can also be used in the lifetime measurements particularly in which various lifetime components can not be successfully resolved.

IV. THEORETICAL CONSIDERATIONS

A. Lifetimes

The lifetime spectrum of positrons in a molecular substances in which Ps is formed consists of three lifetime components, a short-lived component with a meanlife $\tau \approx 0.125$ nsec from annihilation of p-Ps, a component from annihilation of free positrons with $\tau \approx 0.5$ nsec, and a longlived component from pick-off annihilation of o-Ps with $\tau \approx 1-5$ nsec. However, in many substanses the p-Ps annihilation component is often indistinguishable from the free positron annihilation component. Thus in most cases lifetime spectra are decomposed into two lifetime components leaving the short-lived positron states in an unresolved short meanlife component. At present we are more interested in the well defined, long-lived o-Ps component because it contains the most valuable information about the microstructural properties of the sample.

Meanlife of the long-lived o-Ps component in molecular substances was first calculated by Brandt *et al* using the free volume model⁽¹⁶⁾. The o-Ps pick-off rate A_o , the reciprocal of o-Ps pick-off meanlife, can be calculated in terms of the overlap of the positron component of the o-Ps wave function with the lattice wave function, i. e..

$$\lambda_p = \pi r_e^2 c \int_L \varphi_L^*(r) \varphi_{+b}^*(r) \varphi_{+b}(r) \varphi_L(r) dr^3, \quad (5)$$

where r_e is the classical electron radius, 2.8×10^{-13} cm, c is the velocity of light, $\Psi_{+b}(\mathbf{r})$ is the wave function of the positron in the field of the electron to which it is bound as o-PS and the field of the lattice, and $\Psi_L(\mathbf{r})$ is the electron wave function in the lattice L . In order to evaluate equ. (5), the authors of ref. (16) made the following assumptions. (1) The mutual Ps and lattice polarization is neglected; (3) the lattice is represented as region of a rectangular potential of height U_o , radius

(16) W. Brandt, S. Berko, and W.W. Walker, Phys. Rev. 120, 1289 (1960).

r_0 (or "excluded volume" v_0) and electron density ρ_0 , each region being centered in a cell volume v_1 of radius r_1 . For $r_0 \leq r \leq r_1$, $U_1=0$. Thus, the volume v_1-v_0 is the free volume of the cell; (3) the thermalized *o*-Ps atoms are treated in the zero-velocity ($\mathbf{k}_{ps} \approx 0$) approximation. Therefore, equ. (5) is simplified and becomes a problem of evaluating the *o*-Ps density distribution in a lattice, i. e.,

$$\lambda_p = \pi r_0^2 c \rho_0 \int_{v_0} \psi_{ps}^* \psi_{ps} dr^3 \quad (6)$$

Positronium wave functions can be calculated by solving the Schrödinger equations for the excluded and the free volumes for various lattice geometries in the Wigner-Seitz approximation. The result for equ. (6) can be written as

$$\lambda_p = \frac{\pi r_0^2 c \rho_0}{1 + F(U_0, r_0, r_1)}, \quad (7)$$

where the function F is the ratio of *o*-Ps density in the free volume and that in the excluded volume. This simplified free volume model has been useful as a means of describing the observed temperature and pressure dependence of *o*-Ps decay rates in molecular substances, especially in which positronium atoms are highly delocalized. In the case of liquids or amorphous solids in which positronium atoms may be confined in cavities or in less dense regions, the *o*-Ps pick-off rate is now probing the microscopic instead of the usual macroscopic volumetric properties. This special property makes the positron method valuable for investigating phase transitions in molecular solids which will be discussed in detailed later. With some modifications in the original free volume model, the *o*-Ps pick-off rate in molecular solids can be shown to be related to the local microscopic volume change at the defect sites where *o*-Ps atoms annihilate. In this modified free volume model, or cavity model, the volume of a sample is divided into many unit cells with a mean cell volume v . Each unit cell is centered at a cavity site instead of at a lattice site as in the original model. An *o*-Ps atom may occupy any one of the cells. In a unit cell, there is an empty space v_f free of molecular electrons and an excluded volume $v - v_f$ occupied by molecules. The pick-off rate of *o*-Ps in a unit cell can be calculated in the similar manner as in equ. (7), i. e.,

$$\lambda_p = \frac{\lambda_s}{(1 + F)}, \quad (8)$$

where $\lambda_s = \pi r_0^2 c \rho_0$ and F is now evaluated with the new boundary conditions. The difference between this modified model and the original model is that the F function is now dependent on the mean free volume of the cavities which *o*-Ps occupied instead of the macroscopic lattice parameters of the sample. In liquid, Ps is confined in the "Ps bubble". Hence, the free volume in the above calculation should be replaced by the volume of the bubble. The total energy of the bubble consists of the zero point energy of Ps atom, a pressure volume term, and a surface contribution,

$$E = E_0(R) + \frac{3}{4} \pi R^3 P + 4\pi R^2 \sigma, \quad (9)$$

where R is the bubble radius, P is the pressure, and σ is the surface tension. R can be determined by minimization of E with respect to R . This model successfully explains the abnormal change of *o*-Ps lifetime during the solid-liquid phase transition, especially at the ice-water transition where the original free volume model predicted an opposite result.

In addition to *o*-Ps meanlife, another annihilation parameter, the relative intensity of the long lifetime component, I_2 , is also useful. Since statistically 3/4 of positronium atoms formed are in the ortho state, the probability of positronium formation in a sample can be determined from the intensity I_2 if there is no ortho-para conversion or chemical quenching.

At present the process regarding the formation of positronium in molecular solids is still not well understood. The existing models proposed originally for explaining positronium formation in gases and liquids may be applicable in amorphous solids with some modifications. In 1949, Ore first proposed a theoretical model based on energy considerations for evaluation of the probability of positronium formation in gases⁽¹⁷⁾. This is now well known as "Ore Gap" model. The so called "Ore

Gap" is the range of positron energies in which formation of positronium is possible. The lower boundary of the Ore gap E_{min} is the threshold energy for positrons to form positronium which is $V_i - 6.8$ eV. V_i is the ionization potential of a molecule of the medium, and 6.8 eV is the binding energy of positronium. The upper boundary of the Ore gap E_{max} could be V_i or $V_{ex} + V_{ex}$ is the lowest excitation potential of the molecule. If the positron energy $E > V_i$, inelastic scattering with ionization is more likely than positronium formation and if $E > V_{ex}$, the excitation will compete with positronium formation. If one assumes that the spectrum of slow positrons with energies from zero to E_{max} is equally distributed, and that all positrons with energies located in the Ore gap actually from positronium the probability of positronium formation will be given by

$$P = \frac{E_{max} - E_{min}}{E_{max}} = \frac{A}{E_{max}}, \quad (10)$$

where A is the width of the Ore gap. Since E_{max} could be either V_i or V_{ex} , we have P in the range

$$\frac{6.8}{V_i} > P > \frac{V_{ex} - (V_i - 6.8)}{V_{ex}} \quad (11)$$

The Ore gap model is only good for simple gases and needs some modifications for other media in which some of positrons in the Ore gap are slowed down below the Ore gap without formation of positronium. In other words, the validity of the Ore model depends on the competition between the positronium formation and the slowing down process in the Ore gap. Detailed discussion on the Ore model can be found in review articles^(5,17-20).

Recently, a new model, called the spur reaction model, has been proposed by Mogensen to explain the formation of positronium in liquids and solids⁽²¹⁾. At present, the spur model has not yet been well accepted due to the lack of quantitative theoretical proof of the spur reaction. However, this model has been shown to be in agreement with many experimental results for liquids and solids⁽²²⁾. We shall discuss the spur model and compare it with the Ore model.

A "Spur" has been defined in radiation chemistry as "a transient cluster of reactive species, such as one or more ion-electron pairs, formed during the irradiation of a material"⁽²¹⁻²⁴⁾. The "Positron spur" is defined as the cluster of reactive species, such as the positron, ion-electron pairs, and free radicals, formed when the energetic positron loses the last part of its kinetic energy in a material⁽²¹⁾. Positronium is formed by a reaction between the positron and one of the electrons in the positron spur. This process must compete with the recombination of electrons and positive ions and also with the diffusion of electrons out of the spurs. Reactions of the positron and the electrons with the solvent molecules or with scavengers in the spur will also influence the Ps formation. Other factors, such as the solvation and mobilities of the electrons and the positron and chemical reactions between various short-lived species and scavengers in the spur, may also affect the Ps formation. Obviously, it is difficult to perform any quantitative calculation of the probability of Ps formation in the spur taking account of all factors discussed above. A rough estimation of probability P of Ps formation in the spur can be done by considering only the interaction between a pair of thermalized positron and electron in the spur^(20,21,25). The probability for them to escape combination is $\exp(-r_c/r)$, where r is the distance between the pair and $r_c = e^2/\epsilon KT$ is Onsager's critical distance in a medium of dielectric constant ϵ . The probability of Ps formation P is given as

$$P = 1 - \exp(-r_c/r) \quad (12)$$

-
- (17) A. Ore, Univ. i. Bergen Arobok, Naturvitenskap. Rekke, No. 9.
 (18) P.R. Wallace, Solid State Phys. 10, 1 (1960).
 (19) R. A. Ferrell, Rev. Mod. Phys. 28, 308 (1956).
 (20) S. J. Tao, Appl. Phys. 10, 67 (1976).
 (22) H.A. Schwarz, J. Chem. Phys. 55, 3647 (1971).
 (23) J. L. Magee and A. B. Taylor, J. Chem. Phys. 56, 3061 (1972).
 (24) G. Czapski and E. Peled, J. Phys. Chem. 77, 893 (1973).
 (25) W. Brandt, Appl. Phys. 5, (1974).

If the value r , which may be estimated from the size of spurs, is known P can be calculated, and vice versa.

If one considers that around the last ionization site of the positron there are α pairs of electrons and positive ions and some electron scavengers in the spur, the probability of Ps formation in the spur can be estimated to be⁽²⁰⁾

$$P_{s,p} = \frac{\alpha}{\alpha+1} \exp [-(\lambda_f + RN_s)t_c] \left[1 - \exp \left(-\frac{r_c}{r} \right) \right] \quad (13)$$

where λ_f is the annihilation rate of the positron in spur before formation of positronium, R and N_s are the reaction rate and the concentration of the scavenger in the spur, t_c is the time for positronium formation in the spur, and r_c is the Onsager's critical distance defined previously.

Both the Ore gap model and the spur model, even with modifications, can only explain some of the experimental results but not all of them. Apparently, the mechanism for positronium formation in matter contains many "variables", and which variable would be the dominating factor for positronium formation is dependent on individual materials. In the two models discussed above, each considers only one part of the variables. In other words, each has its own merit depending on the individual samples. Certainly, at present one can not discard either model unless a new theory which could take all factors into account for the Ps formation process is developed.

B. Momentum Distributions

As we have mentioned before, the momentum distributions of the annihilating positron-electron pairs can be measured by the twophoton angular correlation method or by the Doppler broadening technique. The momentum distributions observed in many molecular substances generally show a low and a high momentum component^(28,31). The low momentum component, or called narrow component with an intensity I_N is attributed to the self-annihilation of parapositronium. From statistical considerations there are 25% of positronium atoms formed in the singlet state and 75% of them in the triplet state. Hence, one would expect $I_N = I_2/3$, where I_2 is the intensity of the long lifetime component from lifetime measurements, unless there is appreciable ortho-para conversion^(28,30). In this case $I_N > I_2/3$ would result⁽³²⁾. In the case of chemical quenching, I_N would be the same or smaller than the original value depending on the nature of the chemical reactions⁽³³⁾. Therefore, measurements of I_N are useful in the study of inhibition and quenching of positronium in molecular substances⁽⁵⁾. From the width of the narrow component of the angular distributions one can estimate the kinetic energy of p -Ps at the moment of annihilation. In most of molecular liquids and amorphous solids, the experimental results indicate that the kinetic energy of p -Ps is about 0.1-0.3 eV which is much higher than the thermal energy of p -Ps⁽²⁷⁻³⁰⁾. This is due to localization or confinement of p -Ps atoms in the medium as described in the free volume model. Delocalization of p -Ps atoms has been found in single crystals of quartz^(34,37), CaF₂⁽³⁵⁾, and ice⁽³⁸⁾ in which a much smaller width of p -Ps peaks are observed. In additions, a few narrow satellite peaks are also observed simultaneously at the projections of reciprocal lattice vectors onto the measured momentum direction.

The high momentum components in the molecular substances are attributed to the annihilation of free positrons and pick-off annihilation of o -Ps with outer most electrons of the molecules. Unlike

(26) G. Trumpy, Phys. Rev. **118**, 668 (1960).

(27) P. Colombino, B. Fiscella, and L. Trossi, Nuovo Cimento. **38**, 707 (1965).

(28) D. K. Kerr, S.Y. Chuang, and B. G. Hogg, Mol. Phys. **10**, 13 (1965).

(29) S.Y. Chuang and B. G. Hogg, Can. J. Phys. **45**, 3895 (1967).

(30) B. G. Laidlaw, V. I. Goldanskii, and V. P. Shantarovich, At. Energy Rev. **6**, 149 (1968).

(31) R.M. Singru, K.B. Lai, and S. J. Tao, At. Data & Nucl. Tables **17**, 271 (1976).

(32) S.Y. Chuang and S. J. Tao, Appl. Phys. **3**, 199 (1974).

(33) S.Y. Chuang and S. J. Tao, Phys. Rev. **A9**, 989 (1974).

(34) G. Coussot, Phys. Lett. **A30**, 138 (1969).

(35) W. Brandt, G. Coussot, and R. Paulin, Phys. Rev. Lett. **23**, 522 (1969).

(36) A. Greenberger, A. P. Mills, A. Thompson, and S. Berko, Phys. Lett. **A32**, 72 (1970).

(37) C. H. Hodges, B. T. A. Mckee, W. Trifhauser, and A. T. Stewart, Can. J. Phys. **50**, 103 (1972).

(38) O. E. Mogensen, G. Kvajic, M. Eldrup, and M. Milosevic-Kvajic, Phys. Rev. **B4**, 71 (1971).

the momentum distributions in metals which sophisticated calculations have been performed with solids states theories⁽³⁹⁾, very little theoretical studies on the momentum distributions in molecular substances have been performed. Chuang and his coworkers were first to perform momentum distributions calculations for the high momentum components in simple molecules, eg., methane, hexane, decane, and ammonia^(29,40-42). In their calculations, positrons have been assumed to be thermalized before annihilation and the positron-electron correlation has been ignored. Due to molecular disordering in liquids and amorphous solids, the momentum distributions of the annihilating pairs were treated to be isotropic. The spherically averaged momentum distributions, $N(p)$ have been calculated from

$$N(p) = \int_0^\pi X(p)X^*(p) \cdot 2\pi p^2 \sin \theta d\theta, \quad (14)$$

where

$$X(p) = (2\pi)^{-3/2} \int \exp(-i\mathbf{p} \cdot \mathbf{r}) \psi_-(\mathbf{r}) \psi_+(\mathbf{r}) d\mathbf{r}$$

is the Fourier transform of the product of electron wave function $\psi_-(\mathbf{r})$ and the positron wave function $\psi_+(\mathbf{r})$. Electron wave functions for the molecule have been constructed from combinations of SCF atomic orbitals. The positron wave functions corresponding to the individual atomic potential have been calculated using Wigner-Seitz approximation. The electron-positron wave function product for the molecule would then be a combination of products from the individual atoms. Their results indicated that valence electrons in the covalent bonds are responsible for the high momentum components observed in these simple molecules.

In the above calculations, no differentiation is made between the pick-off annihilation of *o*-Ps and the annihilation of free positrons. In general, one would expect that the angular distribution due to pick-off annihilation of *o*-Ps is broader than that from direct annihilation of free positrons^(43,44). However, recent experiments in liquid and solid hydrocarbons⁽⁴⁵⁾ show that there are about 40% of positronium formed in the liquid states ($I_y \approx 10\%$) but none in the solid states ($I_y \approx 0$), and that the high momentum components are practically the same for both liquid and solid states. Other experiments in Teflon of two different degrees of polymer crystallinity⁽⁴⁶⁾ show that there is a large difference in I_y ($\Delta I_y = 6\%$) but no difference in high momentum distributions between these two samples. Since there is no possible mechanism for ortho-para conversion in those experiments, the difference in I_y should be reflected in a threefold difference in *o*-Ps population. Therefore, the results of the above experiments seem to indicate that momentum distributions from *o*-Ps pick-off are similar in shape to those from unbound positrons in the hydrocarbons and Teflon samples investigated. Apparently, more theoretical and experimental studies are needed to clarify this point.

In calculating the positron wave function in molecular systems, Schrader⁽⁴⁷⁾ has gone a step further by constructing the so called positronic molecular orbital (PMO) which is similar to the electronic molecular orbital (EMO). The product of the EMO and PMO is Fourier-transformed into momentum space which is then used to calculate angular correlation curves.

V. PHASE TRANSITIONS IN MOLECULAR SUBSTANCES

A. Solid-Liquid Transitions

Positron annihilation parameters, especially the meanlife of *o*-Ps are sensitive to various phase

- (39) Please see the review article of West (Reference 2) and the papers quoted in Reference 31.
- (40) S. Y. Chuang and B. G. Hogg, *Nuovo Cimento* **58B**, 381 (1968).
- (41) S. Y. Chuang, W. H. Holt, and B. G. Hogg, *Can. J. Phys.* **46**, 2309 (1968).
- (42) W. H. Holt, S. Y. Chuang, A. M. Cooper, and B. G. Hogg, *J. Chem. Phys.* **49**, 5147 (1968).
- (43) F. H. H. Hsu and C. C. Wu, *Phys. Rev. Lett.* **18**, 889 (1967).
- (44) J. D. McGervey and V. F. Walters, *Phys. Rev.* **B2**, 2421 (1970).
- (45) G. DeBlonde, S. Y. Chuang, B. G. Hogg, D. P. Kerr, and D. M. Miller, *Can. J. Phys.* **50**, 1619 (1972).
- (46) I. K. Mackenzie and B. T. A. McKee, *Can. J. Phys.* **44**, 435 (1966).
- (47) D. M. Schrader, *Phys. Rev. A1*, 1070 (1970).

transitions in molecular substances. As we have discussed in the previous sections, these parameters are closely related to the electron density as well as the intermolecular force of the surrounding molecules. If there is a sudden change in the intermolecular force or the electron density in the sample, which usually occurs during phase transitions, then one will observe a sudden change in positron annihilation parameters. Early studies of phase transitions by the positron method were mainly on the solid-liquid phase transition in molecular substances. Among those, the ice-water transition has received a great deal of attention^(49-51,16). In particular, it has been demonstrated in Ref. (51) that at the ice-water phase transition, for both H₂O and D₂O, a discontinuity exists in the lifetime τ_2 and relative intensity I_2 of o-Ps shown in Fig. 9. An abrupt increase in the long lifetime upon melting has also been observed in many molecular substances. Hogg and his coworkers^(42,45,52-53) reported the change in the long lifetime τ_2 during solid-liquid phase change in a number of molecular materials, including ammonia, methane, benzene, cyclohexane, phenol, naphthalene, diphenylamine, *N*-phenylbenzylamine, and *p*-bromotoluene. Chuang and Tao⁽⁵⁴⁻⁵⁵⁾ observed abnormal changes in the long lifetime component upon melting in methanol, deuterated methanol, methyl mercaptan, *n*-tetradecane, *n*-hexadecane, *n*-octadecane and polyethyleneglycols. Kajcsos *et al.*⁽⁵⁶⁾ also measured the positron lifetimes in many hydrocarbons, including eicosane, 3-methylpentane, 2-methylpentane, 2,2-dimethylbutane, 2,3-dimethylbutane, hexane, and Dodecane, and found that most of the lifetime

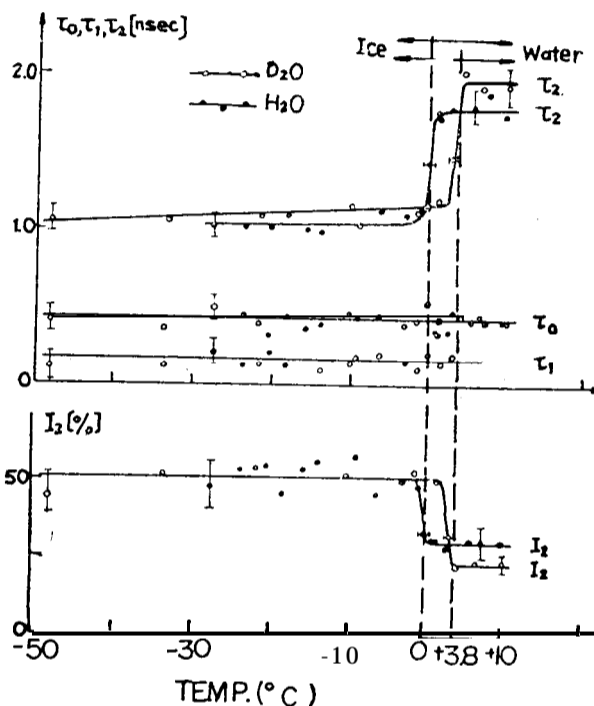


Fig. 9. τ_2 and I_2 for H₂ and D₂O as a function of temperature⁽⁵¹⁾.

- (48) R. L. de Zafra and W. T. Joyner, Phys. Rev. 112, 19 (1958).
 (49) G. Fabri, E. Germagnoli, I.F. Quercia, and E. Turrisi, Nuovo Cimento 30, 21 (1963).
 (50) P. Colombino, B. Fiscella, and L. Trossi, Nuovo Cimento 38, 707 (1965).
 (51) K. Petersen, M. Eldrup and G. Trumpy, Phys. Lett. 31A, 109 (1970).
 (52) E. L. E. Kluth, H. Clarke, and B. G. Hogg, J. Chem. Phys. 40, 3180 (1964).
 (53) A. M. Cooper, G. deBlonde and B. G. Hogg, Phys. Lett. 29A, 275 (1969).
 (54) S.Y. Chuang and S. J. Tao, Phys. Lett. 33A, 56 (1970).
 (55) S. Y. Chuang and S. J. Tao, *Phase Transitions-1973, Proc. of the Conf. on Phase Transition and Their Application in Materials Science*, University Park, Pennsylvania, May 23-25, 1973. p. 363.
 (56) Zs. Kajcsos, I. Dezsi, and D. Horvath, Appl. Phys. 5, 53 (1974).

parameters (τ_2 and I_2) change upon melting and their values are lower in the solid than in the liquid phase. Ito and Tabata⁽⁵⁷⁾ have performed lifetime measurements in liquid and solid amides, including formamide, N-methylacetamide, N, N-dimethylacetamide, acetamine, N-methylacetamide, N,N-dimethylacetamide, and propionamide. They found that the long lifetime τ_2 for the liquid amides is always larger than that for the solids and that the relative intensity I_2 is about twice as large in the solids as in the liquids, independent of the density.

Some important results from the measurements mentioned above can be summarized as follows:

- (1) The long lifetime τ_2 is always longer in the liquid than in the solid for the samples mentioned above. This can be understood as due to the formation of Ps bubble in liquids. The larger the bubble size the longer the o-Ps atom will live according to the free volume model discussed previously. But in the solid, o-Ps is confined in already existing holes or cavities which is normally smaller than the o-Ps bubbles in the liquid. Hence a shorter o-Ps meanlife is observed in the solid than in the liquid. Of course, if the molecular solid contains very large voids such as in the case of silica gels⁽⁵⁸⁻⁶⁰⁾, a very long meanlife of o-Ps in the order of 10~100 nsec may be observed.
- (2) The probability of Ps formation, either obtained from I_2 or from I_Y , does not vary in a simple way from solid to liquid phase for the materials discussed above. In nonpolar molecules, such as most of hydrocarbons, Ps formation probability is much higher in the liquid than in the solid. In particular Ps atoms are not found at all in the solid phase of methane, benzene, and cyclohexane, although a large fraction of Ps atoms are observed in their liquid states⁽⁴⁹⁾. In polar molecules, such as water, methanols, phenol, and amides, the Ps yield is enhanced in the solid compared with the liquid, as shown in Figs. 10 and 11. In some other molecules, such as ammonia, the Ps yield is unchanged over the phase transition. This complicated feature of Ps formation in the solid-liquid phase change can not be explained by the Ore model. The spur reaction model seems to be able to predict the Ps yield in some non-polar and polar molecules during the phase change⁽²¹⁾. For example, in polar molecules, the Ps formation is mainly determined by the solvation and dielectric shielding effects of the positron and electrons according to the spur model. Therefore, to observed higher values of I_2 in the solid than in the liquid phase of water, methanols and amides might be due to a large increase in the solvation time and decrease in the dielectric constant on solidification. However, the abnormal behavior of Ps formation in solid hydrocarbons⁽⁴⁹⁾ can not be clearly predicted by the spur model. At present, one can only speculate that the trapping of positrons and electrons by defects in the solids might play an important role on the formation of positronium in solid media.

B. Liquid-Liquid Transitions

In addition to the Solid-liquid transition, some organic compounds, known as liquid crystals, exhibit liquid-liquid phase transitions. The molecules in liquid crystals are long and rodlike. Between the melting point and the transition point at which the substance becomes isotropic liquid, it has one or more anisotropic mesophases. There are three mesophases, the nematic, cholesteric and smectic phases. In the nematic mesophase, the molecules are able to move around from one region to another as in a liquid but they are parallel to each other with an orientational order. In the cholesteric mesophase, the substance consists of parallel sheets. The molecules are aligned parallel to each other in each sheet. The direction of alignment is different from one sheet to another. In the smectic mesophase, the substance consists of a series of layers, in which the molecules are parallel to each other and normal to the layer plane. Some mesomorphic transitions are enantiotropic. In other words, the transitions are observable on the heating as well as on the cooling cycle. Some are monotropic mesomorphic transitions, which are observed only on cooling.

Positron lifetimes in many liquid crystalline compounds have been investigated by Walker and

(57) Yasuo Ito and Yoneho Tabata, Chem. Phys. Lett. 15, 584 (1972).

(58) S.Y. Chuang and S. J. Tao, J. Chem. Phys. 52, 749 (1970).

(59) S.Y. Chuang and S. J. Tao, J. Chem. Phys. 54, 4902 (1971).

(60) S.Y. Chuang and S. J. Tao, Can. J. Phys. 51, 820 (1973).

his coworkers⁽⁶¹⁻⁶⁵⁾ and by others⁽⁶⁶⁻⁶⁷⁾. Some of the data are listed in Table I. Abrupt changes in the long-lived o-Ps component have been observed at all solid-mesophase transitions and at all mesophase-mesophase transitions in those materials investigated. However, there is only a little or no change in τ_2 upon mesophase-isotropic transitions. The sudden increase in τ_2 at solid-mesophase transitions in liquid crystals is similar in nature to the usual solid-liquid transitions as discussed before. The behavior of o-Ps in the mesophases of liquid crystals can also be described by the bubble model. The o-Ps atoms are most likely confined in the less dense region. The meanlife of o-Ps is of course dependent on the volume or the bubble size where the o-Ps atom is confined. It also depends on the strength of molecular interactions. The confinement of o-Ps in the smectic mesophase are stronger than in the cholesteric or nematic phases and hence τ_2 increases at the smectic-cholesteric and smectic-nematic transitions. The little or no-changes in τ_2 at cholesteric-isotropic and nematic-isotropic transitions indicates that the molecules in the cholesteric or nematic phases already have a lot of freedom that the Ps bubble formation in those mesophases is only a little or no difference from that in the isotropic liquids. In fact, very little changes in entropy and no discontinuity in the surface tensions at mesophase-isotropic transitions are observed^(*).

C. Solid-Solid Transitions

The positron method is also sensitive in detecting the solid-solid phase changes. The most well known materials exhibited solid-solid phase transitions are plastic crystals and polymers. The so called plastic crystals⁽⁶⁹⁾ are globular molecules which are either symmetrical around their center or give a sphere by rotation around an axis. In those molecules the freedom to rotate exists already in the crystal state, but the coherence of the crystal is broken only at a higher temperature, the melting point. In other words, the plastic crystals undergo a change in its crystallographic structure at a certain transition point in the solid state. The crystals are anisotropic at temperatures below the transition point and become isotropic or plastic crystals at temperatures above the transition point. Cooper et al.⁽⁵³⁾ have measured temperature dependence of position lifetimes in a plastic crystal, cyclohexane. Their result shows a large discontinuity in τ_2 at the solid-solid phase transition point, -86°C . Chuang and Tao^(54,55) have studied positron lifetimes in a series of simple plastic crystals, CH_3OH , CD_3OD and CH_3SH , as a function of temperature. It was found that both τ_2 and I_2 undergo an abrupt change at the transition points in those crystals, as shown in Fig. 10 and 11. They also observed an isotropic shift for deuterated methanol in which transition point, -110°C , is 7 degrees higher than that of normal methanol. This confirms that molecular rotation is responsible for the phase transitions in solids. It is also interesting to note that the values of I_2 for methanols starts to increase at a temperature about the degrees below the transition point and reaches a maximum at the transition point. This indicates that the rotation of methyl groups in methanols starts at a temperature, -130°C in CH_3OH and -120°C in CD_3OD , about ten degrees below the transition point. For CH_3SH the transition point, -135°C , is already lower than the rotation temperature of the methyl group, therefore I_2 remains unchanged in the low temperature solid phase up to the transition point. Their results agree well with the linewidth measurements of proton magnetic resonance in CH_3OH and CH_3SH ⁽⁷⁰⁾, as shown in Fig. 11. Walker et al. also observed the solid-solid phase transitions in cyclooctanone⁽⁷¹⁾ and some organic compounds (see Table I). Unlike the small

(61) G. D. Cole and W. W. Walker, J. Chem. Phys. 39, 850 (1963).

(62) G. D. Cole and W. W. Walker, J. Chem. Phys. 42, 1692 (1965).

(63) G. D. Cole, W. G. Merritt, and W. W. Walker, 49, 1980 (1968).

(64) W. G. Merritt, G. D. Cole, and W. W. Walker, Mol. Cryst. Liq. Cryst. 15, 105 (1971).

(65) W. W. Walker and E. L. Mueller, Appl. Phys. 3, 155 (1974).

(66) J. B. Nicholas and H. J. Ache, J. Chem. Phys. 57, 1597 (1972).

(67) J. D. McNutt, W. W. Kinnison and M. D. Searcey, Phys. Rev. B5, 826 (1972).

(68) G. W. Gray, *Molecular Structure and Properties of Liquid Crystals* (Academic Press, London and New York, 1962).

(69) J. Timmermans, J. Phys. Chem. Solids, 18, 1 (1961).

(70) K. Krynicki and J. G. Powles, Proc. Phys. Soc. 83, 983 (1964).

(71) W. W. Walker, W. G. Merritt, and G. D. Cole, Phys. Lett. A40, 157 (1972).

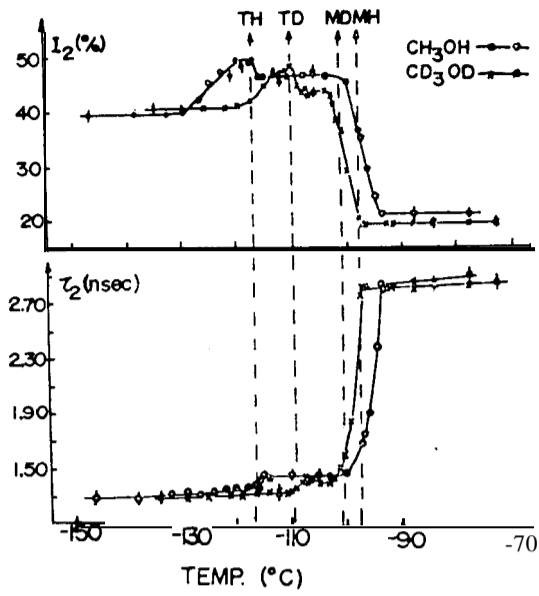


Fig. 10. τ_2 and I_2 for CH_3OH and CD_3OD as a function of temperature.

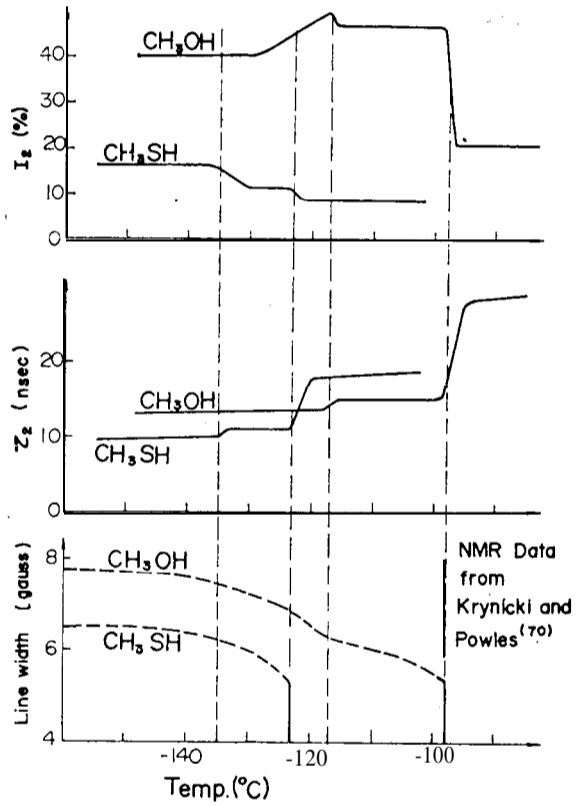


Fig. 11. Comparison of positron parameters with NMR data for detecting phase transitions in CH_3OH and CH_3SH (55).

Table I. The meanlife τ_2 in various phases of some liquid crystals

Compound	τ_2 (nsec) in various phases	Ref.
Cholesteryl acetate	Solid(I) $\xrightarrow{63^\circ\text{C}}$ Solid(II) $\xrightarrow{110^\circ\text{C}}$ Isotropic $\xrightarrow{95^\circ\text{C}}$ cholesteric 1.5 ± 0.1 2.5 ± 0.1 3.2 ± 0.1 3.2 ± 0.1 $\xrightarrow{84^\circ\text{C}}$ Solid(II) 2.5 ± 0.1	(61)
Cholesteryl benzoate	Solid $\xleftarrow{150^\circ\text{C}}$ cholesteric $\xleftarrow{176^\circ\text{C}}$ isotropic 1.3 ± 0.1 3.1 ± 0.1 3.1 ± 0.1 1.4 ± 0.1 2.6 ± 0.1 2.6 ± 0.1	(62) (66)
Cholesteryl butyrate	Solid $\xleftarrow{99^\circ\text{C}}$ cholesteric $\xleftarrow{113^\circ\text{C}}$ isotropic 1.7 ± 0.1 \rightarrow 2.9 ± 0.1 2.9 ± 0.1 1.9 ± 0.1 \leftarrow	(64)
Cholesteryl cinnamate	Solid $\xleftarrow{165^\circ\text{C}}$ cholesteric $\xleftarrow{217^\circ\text{C}}$ isotropic 1.35 ± 0.10 \rightarrow 2.9 ± 0.1 2.9 ± 0.1 1.80 ± 0.10 \leftarrow	(64)
Cholesteric myristate	Solid $\xleftarrow{71^\circ\text{C}}$ smetic $\xleftarrow{76^\circ\text{C}}$ cholesteric $\xleftarrow{81^\circ\text{C}}$ isotropic 1.80 ± 0.10 2.60 ± 0.10 2.70 ± 0.10 2.75 ± 0.10	(66)
Cholesteric propionate	Solid(I) $\xrightarrow{96^\circ\text{C}}$ cholesteric $\xrightarrow{108^\circ\text{C}}$ isotropic $\xrightarrow{108^\circ\text{C}}$ cholesteric 1.6 ± 0.1 3.2 ± 0.1 3.2 ± 0.1 3.2 ± 0.1 $\xrightarrow{88^\circ\text{C}}$ Solid(II) 2.8 ± 0.1	(63)
Cholesteric stearate	Solid(I) $\xrightarrow{83^\circ\text{C}}$ isotropic $\xleftarrow{79.5^\circ\text{C}}$ cholesteric $\xleftarrow{75.5^\circ\text{C}}$ smectic 2.0 ± 0.1 2.9 ± 0.1 2.8 ± 0.1 2.4 ± 0.1 $\xrightarrow{71^\circ\text{C}}$ Solid(II) 2.0 ± 0.1	(62)
p-Azoxyanisole	Solid $\xleftarrow{117^\circ\text{C}}$ Nematic $\xleftarrow{135^\circ\text{C}}$ isotropic (no τ_2) 1.0 ± 0.1 1.0 ± 0.1	(62)
4, 4'-Azoxydianisole	Solid $\xleftarrow{120^\circ\text{C}}$ Nematic $\xleftarrow{136^\circ\text{C}}$ isotropic 1.15 ± 0.10 1.75 ± 0.10 1.85 ± 0.10	(66)
p-Methoxycinnamic acid	Solid $\xleftarrow{175.5^\circ\text{C}}$ Nematic $\xleftarrow{189^\circ\text{C}}$ isotropic 1.20 ± 0.10 2.00 ± 0.10 2.18 ± 0.10	(66)
4-butyloxybenzal-4'-ethylaniiline (BEA)	Solid(I) $\xrightarrow{28.5^\circ\text{C}}$ Solid(II) $\xleftarrow{41.5^\circ\text{C}}$ smetic $\xleftarrow{51.5^\circ\text{C}}$ Nematic 1.25 ± 0.12 1.97 ± 0.05 2.36 ± 0.03 2.72 ± 0.04 $\xleftarrow{66.5^\circ\text{C}}$ isotropic 2.69 ± 0.03	(65)

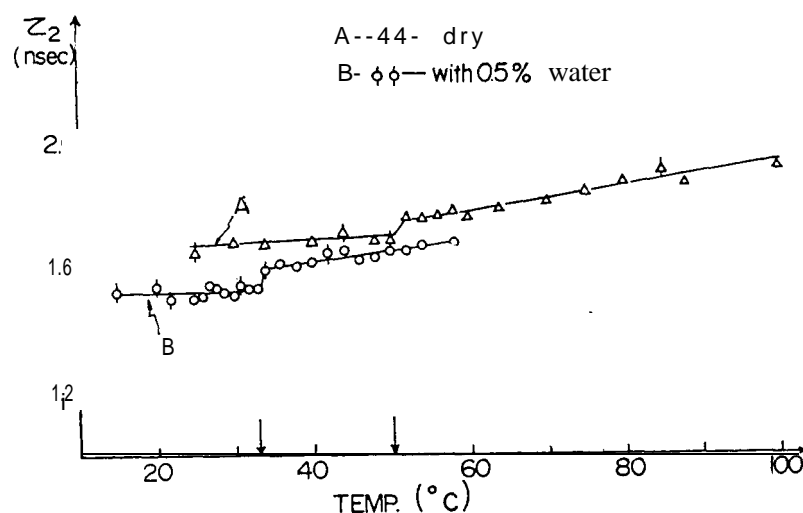


Fig. 12. The meanlife τ_2 of o-Ps annihilation in Nylon 6⁽⁷²⁾.

molecules discussed above, cyclooctanone exhibits thermal hysteresis in the phase transition studies. During the heating cycle from -130°C to 56°C , an abrupt increase in τ_2 was observed between -55°C and -42°C . This represents the transition from a low temperature crystalline form to a high temperature plastic form. Another abrupt change in τ_2 occurs at the solid-liquid transition, between 35°C and 40°C . During the cooling cycle from $+56^\circ\text{C}$ to -130°C , the solid-solid phase change was detected at -106°C . This means that the plastic phase was retained down to -106°C during the cooling cycle. Wang and Ache⁽⁷²⁾ also reported a steep rise in τ_2 between 70°C - 80°C for choline chloride. At this temperature interval the transition from the orthorhombic crystalline form to the disordered cubic form takes place. Goworek and his workers⁽⁷³⁾ have measured the counting rate at the peak of the $2-\gamma$ angular distribution curve, i. e. $N(\theta=0)$, as a function of the temperature of phenanthrene. A change in the peak count $N(\theta=0)$ indicates a change in population of p-Ps in the sample. The value of $N(\theta=0)$ has a sudden increase at 68°C which coincides with the solid-solid phase change in phenanthrene. The melting of the sample also causes a large increase in $N(\theta=0)$. Another example of solid-solid phase transition is the glass transition in polymers which will be discussed in the following section.

VI. GLASS TRANSITION IN POLYMERS

It is known that positronium is formed in organic polymers⁽⁷⁴⁾. The long-lived o-Ps will sense many lattice sites in a polymer before it annihilates. It will probably spend most of its lifetime in a less dense area, or the amorphous region in a polymer. The annihilation of o-Ps in a less dense area will result a characteristic long lifetime component with a meanlife of one to several nanoseconds in the positron lifetime spectrum. The relative intensity of the long lifetime component has been found to be dependent on the fraction of amorphous region in the polymer⁽⁷⁴⁾. The meanlife of the long-lived o-Ps depends on the density of the amorphous region and also depends on the interaction between o-Ps and the surrounding molecules, as we have already discussed in Section IV. Therefore, any microscopic structure change in the amorphous region can be detected by the positron method. In fact, it is one of the most novel methods currently available for studies of polymers, including of morphological properties, polymerization kinetics, molecular weight dependence, molecular motion,

(72) C. Wang and H. J. Ache, J. Chem. Phys. 52, 5492 (1970).

(73) T. Goworek, W. Gustaw, C. Rybka and J. Wawryszczuk, Phys. Stat. Sol. B65, K97. (1974).

(74) S. J. Tao and J. H. Green, Proc. Phys Soc. Lond. 85, 463 (1965).

and glass transition phenomena⁽⁷⁵⁻⁸⁶⁾. In this section, we will only discuss the positron studies on the glass transition in polymers.

Groseclose and Loper⁽⁷⁵⁾ were first to reported that the meanlife of o-Ps in polystyrene and Lucite is sensitive to the change in free volume which occurs at the glass transition. Stevens and Mao⁽⁷⁷⁾ reported that the glass temperature T_g of atactic polystyrene obtained from the positron lifetime measurements is about 13 deg below that measured on a differential scanning calorimeter. After considering the time scale difference between the two experimental methods, they concluded that in its lifetime the o-Ps atom samples the various free volume pockets in the polystyrene favoring those with the larger volumes and hence it is more sensitive to the onset of the segmental motion than experimental techniques which respond to the change in the properties of the sample as a whole. Similar results were also reported for polyisobutylene⁽⁸²⁾. Chuang *et al.*⁽⁷⁹⁾ have investigated the T_g of dried and moist Nylon 6 by the positron lifetime technique. Their lifetime results as shown in Fig. 12 indicate a glass transition at 50° C for dry Nylon and at 33° C for Nylon containing 0.5% water. They also observed that the mean life τ_2 in the dried sample is significantly higher than that in the moist sample at the same temperature. The water molecular absorbed inside Nylon 6 must occupy a part of free volume in the amorphous region where o-Ps occupies and hence the o-Ps meanlife is reduced and the value of T_g is lower in the moist sample.

Although the positron method has shown their sensitivity in detecting T_g in polymers, a question is frequently asked: "What is this method can do that others can not?". It is known that in the glass transition range, many physical properties of the material, including volumetric, thermodynamic, mechanical, and electromagnetic properties, undergo a more or less drastic change. All of these changes have been widely used to determine the glass transition temperature. However, the magnitude of the phenomena associated with T_g decreases with decreasing amorphous content due to the increasing contribution made by the crystalline order to macroscopic properties of the polymers. Therefore, the conventional methods which can be used to determine T_g in wholly amorphous polymers yield less clear results in partially crystalline polymers. For highly crystalline polymers, the glass transition is considered to involve defect regions within or at the boundaries of the lamellae. Therefore, direct determination of T_g in highly crystalline polymers becomes almost impossible for conventional methods. However, such kind of limitation does not exist in the positron method. Although the crystallinity of a sample alters the annihilation characteristic of positrons, the long lived o-PS component always appears even in a highly crystalline polymer due to the fact that most of o-Ps atoms are trapped and annihilate in the defect sites. Therefore, direct determination of T_g in highly crystalline polymers by the positron method is possible and valuable.

To examine that ability of the positron method in detecting the glass transition in highly crystalline polymers, Chuang *et al.* have carefully studies the positron lifetimes in highly crystalline linear polyethylene as a function of temperature⁽⁸¹⁾. The glass transition temperature, T_g , of polyethylene has been a subject of much attention and discussion. The data of T_g reported in the literature span

- (75) B. G. Groseclose and G. D. Loper, Phys. Rev. 137, 939 (1965).
- (76) W. Brandt and I. Spirn, Phys. Rev. 142, 231 (1966).
- (77) J. R. Stevens and A. Mao, J. Appl. Phys. 41, 4273 (1970).
- (78) G. D. Loper, J. P. Wayne, and J. W. Giles Jr. Phys. Lett. 30A, 403 (1969),
- (79) S. Y. Chuang, S. J. Tao, and J. M. Wilkenfeld, J. Appl. Phys. 43, 737 (1972).
- (80) Y. Ito, S. Katsura, and Y. Tabata, J. Polymer Sci. A-2, 9, 1525 (1971).
- (81) M. N. G. A. Khan, J. Phys. D. (Appl. Phys.) 3, 663 (1970).
- (82) J. R. Stevens and R. M. Rowe, J. Appl. Phys. 44, 4328 (1973).
- (83) A. E. Hamielec, M. Eldrup, O. Mogensen, and P. Jansen, J. Macromol. Sci-Revs. Macromol. Chem. C9(2), 305 (1973).
- (84) S.Y. Chuang and S. J. Tao, J. Appl. Phys. 44, 5171 (1973).
- (85) A. Ogata and S. J. Tao, J. Appl. Phys. 41, 4261 (1970).
- (86) S.Y. Chuang, S. J. Tao and T. T. Wang, Macromol 10, 713 (1977).

a rather wide range from 140 to 340° K with most frequent reports centered around 150 and 250°K⁽⁸⁷⁻⁸⁹⁾. This situation exists because of the difficulty of the conventional techniques to determine T_g in highly crystalline polymers as we have just discussed. Among the four linear polyethylene samples under investigation, two of them were Grex 60-002E linear polyethylene having a number averaged molecular weight (M_n) of 11600 and the other two were highly linear polyethylene polywax 1000 and 2000 having a molecular weight (M_n) of 1000 and 2000, respectively. The polymax samples have narrow molecular weight distributions and high degrees of crystallinity, about 0.96-0.97. The degree of crystallinity for the Grex 60-002E samples are 0.68 and 0.77 respectively. Fig. 13 shows values of the decay rate $\lambda_2 (=1/\tau_2)$ of the long lifetime component for polyethylene samples at various temperatures. All λ_2-T curves undergo a change in slope at 150-160° K and also at 230° K. If the discontinuity of λ_2 in the transition region, 150-230°K, is disregarded, the change of λ_2 with temperature resembles the change of density with temperature⁽⁸⁹⁾. For comparison, thermal expansion curves for linear polyethylene samples with various degrees of crystallinity measured by Stehling and Mandelkern⁽⁸⁹⁾ are shown in Fig. 14. The major difference between the positron data and the thermal expansion data is that the slopes of λ_2-T curves outside the transition region are not affected by the crystallinity of the samples, while the thermal expansion coefficient obtained from Fig. 14 is dependent on the degree of crystallinity. This is expected as we have emphasized previously that the free volume change probed by *o*-Ps is a microscopic property near the place where *o*-Ps annihilates instead of a macroscopic volumetric properties.

It is interesting to note that in Fig. 13 the transition begins at about 150° K which coincides with the γ relaxation observed by thermal expansion⁽⁸⁹⁾ and other methods⁽⁹⁰⁾, and that the higher

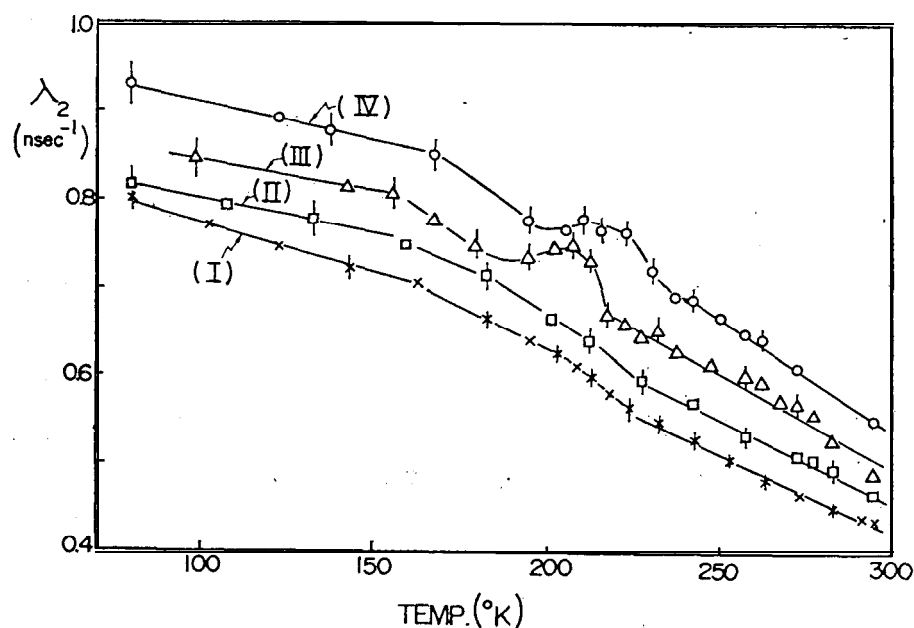


Fig. 13. The annihilation rate λ_2 of the long lifetime component as a function of temperature in linear polyethylene samples⁽⁸⁶⁾.

- (I) Grex 60-002E (deg. of crystallinity=0.68)
- (II) Grex 60-002E (deg. of crystallinity=0.77)
- (III) Polywax 1000,
- (IV) Polywax 2000

(87) R. F. Boyer, *Macromolecules-Reviews* 6, 288 (1973).

(88) G. T. Davis and R. F. Eby, *J. Appl. Phys.* 44, 4274 (1973).

(89) F. C. Stehling and L. Mandelkern, *Macromolecules* 3, 242 (1970).

(90) Please see the review article of R. F. Boyer. *Plast Polym.* 41, 15 (1973).

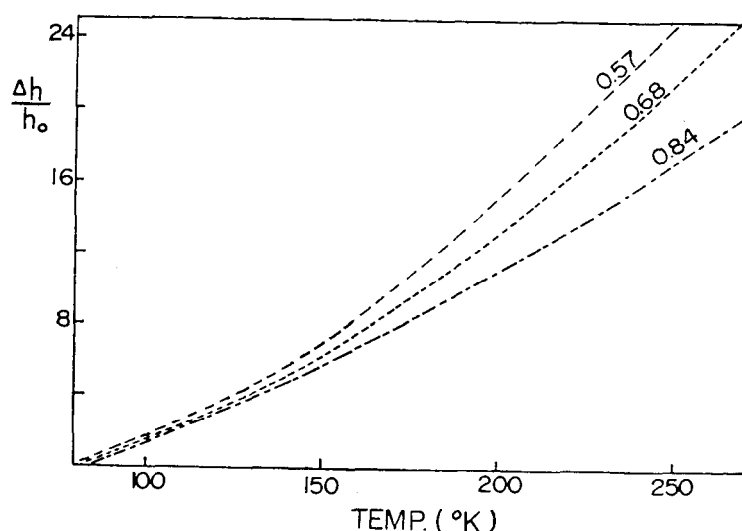


Fig. 14. Thermal expansion curves for linear polyethylene⁽⁹⁹⁾.

limit of the transition, 230°K, coincides with the T_g reported by Davis and Eby⁽⁸⁸⁾ and others⁽⁹⁷⁾. The irregular change of λ_2 for the Polywax samples in the transition region 200-230° K might be due to molecular motions in amorphous regions. Such molecular motions has been reported by McCall and Douglass⁽⁹¹⁾ in their NMR studies on linear polyethylene. They found that the liquid-like motions of the amorphous chains attain an average frequency of 3×10^7 Hz at about 240° K. This frequency is comparable to λ_2 , therefore the annihilation pattern of o-Ps may be altered. The onset of such molecular motion will cause the diffusion of electron density into the free volume where o-Ps occupies. This results a shower reduction or even increase of λ_2 against temperature. As temperature is increased further, the positronium pressure may cause a sudden increase in free volume if the surrounding chain segments become flexible enough. This would induce a drop in λ_2 - T curves. Above this temperature, λ_2 again follows the pattern of free volume change against temperature. The irregularity of λ_2 in the Grex samples is not as pronounced as in the Polywax samples. This is because that the Polywax samples have narrower defect distributions due to their narrow molecular weight distributions and very small amorphous fractions (3 to 4%). A more complex amorphous structure with a broader distribution of defects can be expected in the less crystalline and highly polydisperse Grex samples, consequently the above mentioned effect of molecular motion may take place more smeary in the λ_2 - T curves of Grex samples.

The work on linear polyethylene samples has demonstrated that the long lifetime component of the positron lifetime spectra reveals microscopic structure changes in amorphous region of polyethylene. Therefore, the positron method is a valuable tool to complement other methods for the study of the nature of the glass transition in partially crystalline polymers.

ACKNOWLEDGEMENTS

The author is grateful to S. J. Tao for many years of fruitful collaboration and to P. K. Tseng, F. H. Hsu, G. J. Jan, S. F. Chen and H. J. Ting for their assistance in preparing this paper. This work is partially supported by the National Science Council of Republic of China.

(91) D. W. McCall and D. C. Douglass, *Polymer* 4, 433 (1963).